

# Deciphering the mechanism of human carbonic anhydrases inhibition with sulfocoumarins: computational and experimental studies.

Alessio Nocentini,<sup>[a,b]</sup> Fabrizio Carta,<sup>[b]</sup> Muhammet Tanc,<sup>[b]</sup> Silvia Selleri,<sup>[b]</sup> Claudiu T. Supuran,<sup>[b]</sup> Carla Bazzicalupi,<sup>\*[c]</sup> Paola Gratteri<sup>\*[a]</sup>

**Abstract:** The reaction mechanism of the carbonic anhydrase-mediated hydrolysis of sulfocoumarins to sulfonic acids has been investigated on an enzyme cluster model using the B3LYP hybrid density functional theory (DFT) and the QST procedure for the Transition State (TS) search. A multistep process was highlighted, with the rate determining step identified in the initial dual nucleophilic/acidic attack of the zinc bound-hydroxide ion to the sulfocoumarin sulfur atom and to the C3-C4 double bond. The reported multi-step process, combined to SAR analysis on a new set of derivatives, highlighted unprecedentedly considered mechanistic aspects of the CA-mediated prodrug activation, which in turn do possess relevant consequences to the isoforms-selective inhibition profiles reported by such a class of compounds.

The discovery of the coumarin bioisosters 1,2-benzoxathiine-2,2-dioxides, also named sulfocoumarins, as novel and selective inhibitors of the zinc metalloenzymes  $\alpha$ -carbonic anhydrases (CAs, EC 4.2.1.1) is the result of intense efforts towards the development of innovative compounds as potential tools for the treatment of various diseases.<sup>[1-4]</sup> The role of CAs in cells as well as in complex organisms, is primarily related to their ability to reversibly catalyze the carbon dioxide hydration reaction to afford bicarbonate and a proton.<sup>[5,6]</sup> Such an equilibrium is crucial for a vast array of physio/pathological processes.<sup>[5-7]</sup> The CA mediated catalytic pathway proceeds at first with the nucleophilic attack of a  $Zn^{2+}$ -bound hydroxide ion towards the  $CO_2$  substrate with consequent formation of a  $CA-HCO_3^-$  adduct, which is then displaced from the active site by an additional water molecule. The final, rate limiting step, regenerates the catalytically active  $Zn^{2+}$ -bound hydroxide

ion by means of a proton transfer reaction from the  $Zn^{2+}$ -bound water molecule to an external proton acceptor or to an active site residue.<sup>[7]</sup>

Besides the hydration on  $CO_2$ , some CAs are endowed with a certain substrate versatility, which includes COS,  $CS_2$  cyanamides and aldehydes hydration reactions.<sup>[5]</sup>  $\alpha$ -CAs are also reported to possess hydrolytic activities towards esters of carboxylic acids, sulfonic acids, phosphates and thioesters.<sup>[5,8]</sup>

The esterase activity shown by the  $\alpha$ -CAs, was the enzymatic blueprint which allowed us to make use of prodrugs of the coumarin and sulfocoumarin type as novel classes of CA Inhibitors (CAIs).<sup>[1,9-12]</sup> In analogy to the coumarins, the sulfocoumarins are not *per se* able to inhibit the CA activity. Instead they interfere with the enzyme by acting as efficient substrates for the esterase (sulfatase) activity, generating the actual inhibitor *in situ*.<sup>[1-3]</sup> Thereafter the formed sulfonic acid inhibit the enzyme by means of a stable adduct and a particular inhibition mechanism, i.e., anchoring to the non-protein zinc ligand.<sup>[1-3]</sup> The prodrug features of the sulfocoumarin scaffold was also consistent

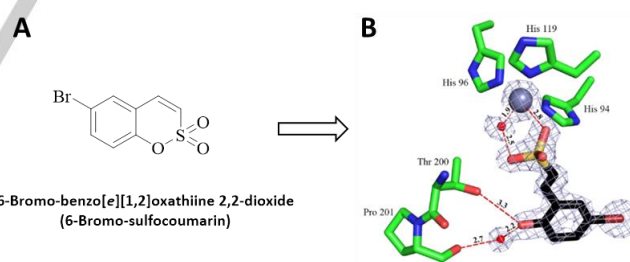


**Figure 1.** A) Structure of the 6-bromosulfocoumarin; B) The corresponding sulfonic acid was obtained from *in situ* hydrolysis and binds into the hCA II/IX mimic active site, by anchoring of the sulfonic acid group to the zinc-coordinated water molecule (PDB 4BCW).<sup>[1]</sup>

with the longer time of incubation required to exert *in vitro* inhibition against the  $\alpha$ -CAs (6h vs 15 minutes for the classical zinc binders CAIs of the sulfonamide type).<sup>[1,9,12]</sup>

Evidences for the CA promoted intramolecular sulfonic ester cleavage was obtained by means of X-ray co-crystallographic experiments conducted by soaking a hCA II/IX mimic isoform with the 6-bromo-sulfocoumarin **1** (Figure 1).<sup>[1]</sup>

The  $2F_o - F_c$  density maps showed a well-defined density for the *in situ* formed sulfonate, which anchors to the Zn-bound

[a] Dr. A. Nocentini, Prof. P. Gratteri  
Department NEUROFARBA – Pharmaceutical and nutraceutical section; Laboratory of Molecular Modeling Cheminformatics & QSAR, University of Firenze, via Ugo Schiff 6, 50019 Sesto Fiorentino (Italy).  
E-mail: paola.gratteri@unifi.it

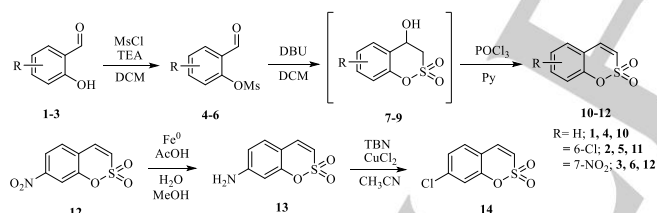
[b] Dr. A. Nocentini, Dr. F. Carta, Dr. M. Tanc, Prof. S. Selleri, Prof. C.T. Supuran  
Department NEUROFARBA – Pharmaceutical and nutraceutical section, University of Firenze, via Ugo Schiff 6, 50019 Sesto Fiorentino (Italy)

[c] Prof. C. Bazzicalupi  
Department of Chemistry "U. Schiff", University of Florence, Via della Lastruccia 3, 50019 Sesto Fiorentino (Italy).  
E-mail: carla.bazzicalupi@unifi.it

water within the hCA II/IX mimic active site.<sup>[1]</sup> The adduct is further stabilized by means of a network of hydrogen bonds occurring between the ligand and the Pro202/Thr200 amino acid residues from the enzyme active site.<sup>[1]</sup>

To date a detailed reaction mechanism for the CA-mediated intramolecular sulfonic esters hydrolysis has not yet been reported. In recent studies, we investigated a variety of sulfocoumarins bearing electro-withdrawing (EWG) or electro-donating (EDG) groups placed at the 6- and 7-position.<sup>[1-3,13,14]</sup> Herein, as extension of our previous investigations, we report novel analogues decorated at the 6- and 7-position with chemical moieties endowed with different electronic properties (EWG and EDG, scheme 1) and their inhibition profiles against the most relevant human (h)CAs are reported. Since computational studies are validated tools to provide deep insights into enzymatic mechanisms,<sup>[15-20]</sup> we made use of the B3LYP hybrid density functional theory (DFT) to study the hydrolysis of the unsubstituted sulfocoumarin (compound **10** – scheme 1) upon the CA-esterase activity, by using the X-Ray crystal structure of CA II/IX mimic in complex with the hydrolysed 6-bromosulfocoumarin as a model.

The novel sulfocoumarins **10-14** were obtained by applying the general synthetic strategy firstly reported by Zalubovski's group (Scheme 1).<sup>[4,13]</sup>



**Scheme 1.** General synthetic procedure of sulfocoumarins **10-14**.

Reaction of the proper 2-hydroxybenzaldehydes **1-3** with mesyl chloride afforded the mesylate derivatives **4-6**, which were treated with 1,8-diazabicyclo[5.4.0]undec-7-ene (DBU), with formation of the racemic 4-hydroxy-3,4-dihydro-sulfocoumarins **7-9** in mixture with their dehydration products **10-12**. The dehydration was further pushed forwards by treating the mixtures with POCl<sub>3</sub> in pyridine. 7-NH<sub>2</sub>-sulfocoumarin **13** was obtained by reducing the correspondent nitro-derivative **12** with iron (0), which in turn was converted to the chlorine compound **14** through Sandmeyer reaction with CuCl<sub>2</sub> in the presence of *tert*-butyl nitrite.

The final compounds **10-14** were screened in vitro for the inhibition against four physiologically relevant hCA isoforms, the cytosolic hCA I and II and the transmembrane tumor-associated hCA IX and XII.

**Table 1:** Inhibition data of hCA isoforms I, II, IX and XII with sulfocoumarins **10-14** compared to the standard sulfonamide inhibitor acetazolamide (AAZ) by the stopped flow CO<sub>2</sub> hydrase assay.<sup>[21]</sup>

Cmp	R	K <sub>i</sub> (nM) <sup>a</sup>			
		hCA I	hCA II	hCA IX	hCA XII
<b>10</b>	H	>100000	>100000	432.2±33.1	69.5±5.1
<b>A<sup>b</sup></b>	6-NO <sub>2</sub>	92000±4800	>100000	3770±240	3160±210
<b>B<sup>c</sup></b>	6-NH <sub>2</sub>	6780±560	8890±710	46.0±3.1	23.0±1.2
<b>11</b>	6-Cl	>100000	>100000	136.3±7.5	89.5±5.4
<b>12</b>	7-NO <sub>2</sub>	>100000	>100000	37.0±2.1	81.7±4.3
<b>13</b>	7-NH <sub>2</sub>	>100000	>100000	33.5±1.9	38.4±2.2
<b>14</b>	7-Cl	>100000	>100000	33.7±1.8	60.9±4.6
<b>AAZ</b>	-	250±15	12±0.8	25±1.4	5.7±0.5

a. Inhibition data are expressed as means ± SEM of 3 different assays; b. compound **10** in ref. 1; c. compound **11** in ref. 1.

The following Structure-Activity-Relationships (SARs) can be drawn from the inhibition data of Table 1:

(i) In agreement with previous literature reports,<sup>[1-4]</sup> the sulfocoumarins **10-14** were ineffective in inhibiting the isoform hCA I and II. The only exception was the compound **B** which was effective against both cytosolic isoforms at low micromolar concentrations (K<sub>i</sub>s 6780±560 and 8890±710 μM respectively).

(ii) The transmembrane hCA isoforms resulted inhibited by the sulfocoumarins here reported, with K<sub>i</sub> values spanning between 33.5±1.9 - 3770±240 nM and 23.0±1.2 - 3160±210 nM against the hCA IX and hCA XII respectively. The introduction of substituents of the NO<sub>2</sub> or NH<sub>2</sub> type on the 6 position of the sulfocoumarin ring, as in **A** and **B**,

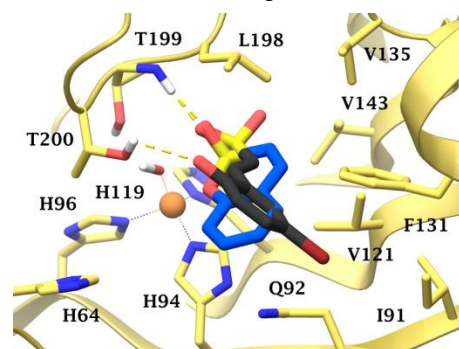


**Figure 2.** Superimposition of the docked pose of sulfocoumarin **10** (blue) and the hydrolyzed form of 6-bromosulfocoumarin (black) in hCA II/IX mimic active site (4BCW).

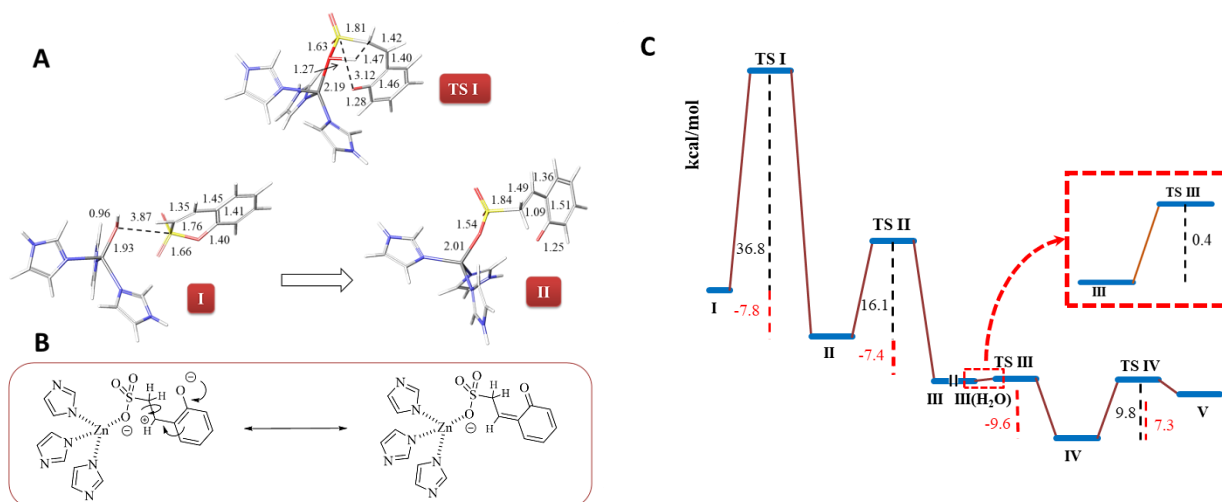


**Figure 3.** A. Reaction path for step I. Thr199 omitted for clarity; B. Drawings of the resonant structures for II. Zinc coordination bonds are represented as hashed lines; C. Energy profile for the calculated multi-step reaction path of the unsubstituted sulfocoumarin CA-mediated hydrolysis. Red dashed lines represent reaction energies, black dashed lines activation energies (energy values in kcal/mol).

led to opposite changes in the hCA IX and XII inhibitory properties in comparison to the unsubstituted **10** ( $K_{\text{is}}$  of  $432.2 \pm 33.1$  and  $69.5 \pm 5.1$  nM, respectively). Indeed, **A** inhibit both isozymes with  $K_{\text{is}}$  ranging between  $3160 \pm 210$  and  $3770 \pm 240$  nM, whereas **B** exhibited enhanced inhibition profiles in the range  $23.0 \pm 1.2$  -  $46.0 \pm 3.1$  nM. Among 7-substituted derivatives, all functionalizations do increase hCA IX inhibition potency with respect to **10**, with hCA XII being instead more significantly affected uniquely in the case of **13** (7-NH<sub>2</sub>,  $K_{\text{i}}$  of  $38.4 \pm 2.2$  nM).

The cluster-based approach was considered to overcome the complexity in treating the overall enzyme systems with the quantum-mechanical (QM) transition state search methods.<sup>[17-19]</sup> It is worth stressing the importance of the identification of a proper cluster model, which was propaedeutical to unveil the reaction mechanism.<sup>[17-19]</sup> Indeed, considering that the differently substituted sulfocoumarins possessed diverse activity on the CA isoforms, we had to look for the common elements deemed to be involved in the esterase process among the different isozymes, whose active site cavities differ for residues composition and molecular architectures.<sup>[5,7,22]</sup> As a result, these latter define lightly narrower binding pockets for hCA I, II in comparison to hCA IX and XII.<sup>[22]</sup>

Thus, a model of the active site was built using the PDB 4BCW coordinates, which includes the essential parts involved in the reaction: (i) the Zn ion; (ii) the Zn-bound OH<sup>-</sup> (as present in the active form of the enzyme); (iii) three imidazole rings representative of the three side chains of the His residues; (iv) the truncated Thr199 residue, that in

the crystal structure established a H-bond with the sulfonate moiety, and (v) an additional water molecule extrapolated from the X-ray structure. In the crystal structure, the hydrolysed 6-substituted sulfocoumarin locates its sulfonate oxygen 2.8 Å apart from the Zn ion. The unsubstituted sulfocoumarin **10** was considered as the best candidate to initially identify the steps through which the process takes place, owing to minor electronic effects by absence of appended substituents. Compound **10** was docked into the 4BCW active site (Figure 2), and subsequently the complex was superposed with the built cluster model to obtain the starting position of **10** into the model system. The transition state (TS) search undertaken (ESI, Theoretical studies) highlighted the presence of a multi-step process (Figure 3).

(i) In the optimized docked pose of the sulfocoumarin **10** within the cluster model (I, cfr ESI for the procedure used to obtain the I, II and TS I systems, i.e. adduct, structures), the distance between the negative oxygen atom of the Zn-bound hydroxide ion and the sulfonate ester sulfur atom was of 3.87 Å (Figure 3A). Such a distance makes the hydroxide ion suitable to elicit a nucleophilic attack towards the electrophilic sulfonic ester, thus inducing the cycle to open by lengthening the distance between sulfur and the endocyclic oxygen. At the same time the hydroxide hydrogen protonates the double bond of the forming ethenylsulfonic acid, with the formation of the stable carbocation locating the positive charge on C4 of the starting sulfocoumarin. The simultaneous occurring of these two events provides the molecule with the degree of

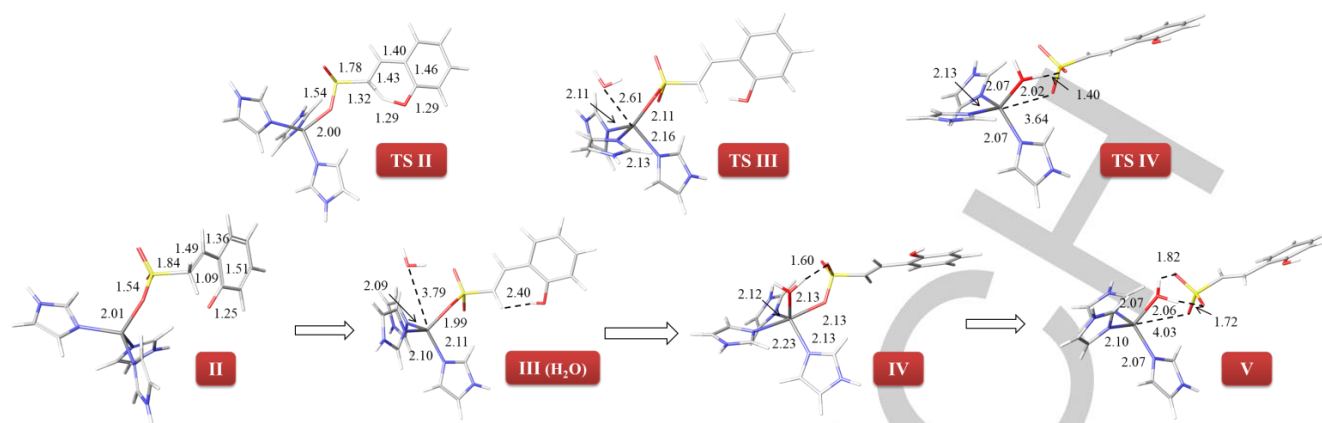


**Figure 4.** Reaction path for steps II, III and IV. Thr199 omitted for clarity. Intermediate III reported as III (H<sub>2</sub>O) for clarity.

freedom necessary to rearrange, leading to the first reaction intermediate (II). The bond lengths featuring II, are consistent with its stabilization by means of two main resonance structures of the carbocation and the phenoxide ion type (Figure 3B). The activation barrier for the first step was 36.8 kcal/mol (Figure 3C).

(ii) The second step pertains the Z to E isomerization (Figure 4). In this step an intramolecular acid-base reaction occurs, where the phenoxide moiety acts as a base to deprotonate the CH<sub>2</sub> moiety (C3 position of the starting sulfocoumarin **10**). As for step (i), also here a simultaneous intramolecular rearrangement takes place, providing the less hindered isomer E (III). Overall, the II → III reaction energy is -7.4 kcal/mol (Figure 3C), while the activation barrier is 16.1 kcal/mol.

(iii) As known, the displacement of a zinc-bound ligand in the enzyme active site proceeds through the so-called water-exchange pathway.<sup>[5]</sup> Thus, an additional water molecule was added to III (ESI, Theoretical Studies). The observed TS evidences that the added water molecule approaches the Zn ion, eliciting a reorganization of the coordination sphere, by which a trigonal bipyramid is formed having the sulfonate oxygen, and its opposite histidine nitrogen in apical positions (Figure 4). The activation barrier is only 0.4 kcal/mol (Figure 3C).

(iv) Finally, the sulfonate moiety slightly moves away from the Zn ion and the remaining components of the trigonal bipyramid rearrange forming a pseudo tetrahedral coordination system (Figure 4). The activation barrier for this step was 9.8 kcal/mol. The anchoring of the sulfonate to the zinc coordinated water molecule is expected to prevent its deprotonation and, as a consequence, the

restoring of the zinc bound hydroxide ion. Noteworthy, it should be mentioned that in the native CA II crystal structure (PDB 2CBA)<sup>[23]</sup> a zinc-bound water molecule has been observed.

The energy profile shown in Figure 3C evidences that product V is thermodynamically unstable with respect to its precursor IV by 7.3 kcal/mol. These data are in agreement with the cluster model herein considered where the bipyramidal coordination of IV is expected to prevail on the pseudo tetrahedral one of V. Nevertheless, it is noteworthy that even in the 4BCW adduct, the coordination geometry of the zinc ion is actually better described as a distorted tetrahedron rather than as a trigonal bipyramid, with an oxygen atom from the hydrolysed inhibitor at only 2.8 Å from the metal centre. Indeed, the relative instability ascribed to the pseudo-trigonal bipyramid coordination pattern found for the adduct IV is compensated by additional non-bonded interactions (i.e. H-bonds and hydrophobic contacts) occurring between the ligand and the amino acid residues of the enzymatic cleft, thus contributing to further stabilize the orientation assumed by the ligand (Figure 2).

In conclusion, our theoretical model indicated the first step, (i.e. the nucleophilic attack of the zinc-hydroxide ion on the cyclic sulfonate), as the rate-determining step for the entire hydrolytic reaction. This finding is not surprising, as the cycle opening and the overall ligand rearrangement required a dual attack of the zinc-bound O-H group both to the sulfocoumarin sulfur atom and to the C3-C4 double bond. Structure-activity-relationship (SAR) analysis based on the obtained inhibition assay was rather flat. We propose that the CA isoform-selective inhibition of sulfocoumarins may be properly ascribed to the mechanism

through each  $\alpha$ -CA hydrolyzes different substrates rather to depend from conventional enzyme-ligand interactions occurring between the amino acids of the enzymatic cleft and the product obtained from the hydrolytic process. In this context, it is reasonable to hypothesize that the ligand rearrangements described in the reaction mechanism (cluster model) strictly depend on the active sites architectures when taking place within the overall binding cavities. As a results, the overall molecular architectures as well as the different isoforms binding site residues could allow or impair the hydrolytic process, with the roomier active site of hCA IX and XII in comparison to hCA I and II being more suitable to accommodate the ligand rearrangements required to start and complete the process.<sup>[5,7,22]</sup> Therefore, the knowledge of such mechanism might further aid in the design of novel specific enzymatic modulators and currently further studies are ongoing in this direction.

## Acknowledgements

This work was supported by the EU FP7 ITN Project Dynano (to M.T. and C.T.S.) and by grants from the University of Florence (Ateneo 2016). The PhD fellowship for A.N. was funded by University of Florence.

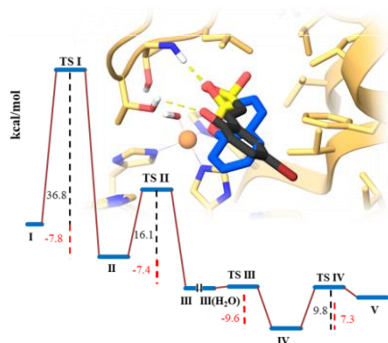
## Conflicts of interest

The authors state no conflicts of interest.

**Keywords:** Carbonic Anhydrase, sulfocoumarin, selective inhibition, reaction mechanism, quantum-mechanics.

- [1] K. Tars, D. Vullo, A. Kazaks, J. Leitans, A. Lends, A. Grandane, R. Zalubovskis, A. Scozzafava, C. T. Supuran, *J. Med. Chem.* **2013**, *56*, 293-300.
- [2] A. Grandane, M. Tanc, L. Di Cesare Mannelli, F. Carta, C. Ghelardini, R. Zalubovskis, C. T. Supuran, *J. Med. Chem.* **2015**, *58*, 3975-3983.
- [3] A. Grandane, M. Tanc, R. Zalubovski, C. T. Supuran, *Bioorg. Med. Chem.* **2014**, *22*, 1522-1528.
- [4] A. Grandane, S. Belyakov, P. Trapencieris, R. Zalubovskis, *Tetrahedron*, **2012**, *68*, 5541-5546.
- [5] V. Alterio, A. Di Fiore, K. D'Ambrosio, C. T. Supuran, G. De Simone, *Chem. Rev.* **2012**, *112*, 4421-4468.
- [6] C. T. Supuran, *Nat. Rev. Drug Discovery*, **2008**, *7*, 168-181.
- [7] C. T. Supuran, *Biochem. J.* **2016**, *473*, 2023-2032.
- [8] M. Tanc, F. Carta, A. Scozzafava, C. T. Supuran, *ACS Med. Chem. Lett.* **2015**, *6*, 292-295.
- [9] A. Maresca, C. Temperini, H. Vu, N. B. Pham, S. A. Poulsen, A. Scozzafava, R. J. Quinn, R. J., C. T. Supuran, *J. Am. Chem. Soc.* **2009**, *131*, 3057-3062.
- [10] A. Maresca, C. Temperini, L. Pochet, B. Masereel, A. Scozzafava, C. T. Supuran, *J. Med. Chem.* **2010**, *53*, 335-344.
- [11] C. T. Supuran, *J. Enzyme Inhib. Med. Chem.*, **2016**, *31*, 345-360.
- [12] F. Carta, A. Maresca, A. Scozzafava, C. T. Supuran, *Bioorg. Med. Chem. Lett.* **2012**, *22*, 267-270.
- [13] M. Tanc, F. Carta, A. Scozzafava, C. T. Supuran, *Org. Biomol. Chem.*, **2015**, *13*, 77-80.
- [14] A. Nocentini, M. Ceruso, F. Carta, C. T. Supuran, *J. Enzyme Inhib. Med. Chem.* **2016**, *31*, 1226-1233.
- [15] G. Tian, Y. Liu, *Phys. Chem. Chem. Phys.*, **2017**, *19*, 7733-7742.
- [16] P. Janoš, T. Trnka, S. Kozmon, I. Tvaroška, J. Koča, *J. Chem. Theory Comput.*, **2016**, *12*, 6062-6076.
- [17] P. Georgieva and F. Himo, *Chem. Phys. Lett.* **2008**, *463*, 214-218.
- [18] V. Pelenschikov, M. R. Blomberg, J. Siegbahn, *Biol. Inorg. Chem.*, **2002**, *7*, 284-298.
- [19] V. Navrátil, V. Klusák, L. Rulíšek, *Chemistry*, **2013**, *19*, 16634-16645.
- [20] R. Z. Liao, J. G. Yu, F. Himo, *J. Phys. Chem. B.* **2010**, *114*, 2533-2540.
- [21] R. G. Khalifah, *J. Biol. Chem.* **1971**, *246*, 2561-2573.
- [22] V. Alterio, M. Hilvo, A. Di Fiore, C. T. Supuran, P. Pan, Parkkila, A. Scaloni, J. Pastorek, S. Pastorekova, C. Pedone, A. Scozzafava, S. M. Monti, G. De Simone, *Proc. Natl. Acad. Sci. U.S.A.* **2009**, *106*, 16233-16238.
- [23] K. Hakansson, M. Carlsson, L. A. Svensson, A. Liljas, *J. Mol. Biol.* **1992**, *227*, 1192-1204.

The reported multistep process for the carbonic anhydrase-mediated hydrolysis of sulfocoumarins highlighted unprecedentedly considered mechanistic aspects of the CA-mediated prodrug activation.



*Alessio Nocentini, Fabrizio Carta, Muhammet Tanc, Silvia Selleri, Claudiu T. Supuran, Carla Bazzicalupi, \*Paola Gratteri\**

**Page No. – Page No.**

**Deciphering the mechanism of human carbonic anhydrases inhibition with sulfocoumarins: computational and experimental studies.**

WILEY-VCH